

This work was written as part of one of the author's official duties as an Employee of the United States Government and is therefore a work of the United States Government. In accordance with 17 U.S.C. 105, no copyright protection is available for such works under U.S. Law.

Public Domain Mark 1.0

<https://creativecommons.org/publicdomain/mark/1.0/>

Access to this work was provided by the University of Maryland, Baltimore County (UMBC) ScholarWorks@UMBC digital repository on the Maryland Shared Open Access (MD-SOAR) platform.

**Please provide feedback**

Please support the ScholarWorks@UMBC repository by emailing [scholarworks-group@umbc.edu](mailto:scholarworks-group@umbc.edu) and telling us what having access to this work means to you and why it's important to you. Thank you.

## RESEARCH ARTICLE

10.1002/2016JD026265

## Key Points:

- Satellite data are used to evaluate the variability of the diurnal cycle (DC) of the surface temperature on the decadal timescale
- It is found that the diurnal temperature range (DTR) of the surface skin temperature over the global Earth has currently positive trend
- A possible cause of observed DTR increase is a decrease of the night cloud cover

## Correspondence to:

A. Ruzmaikin,  
alexander.ruzmaikin@jpl.nasa.gov

## Citation:

Ruzmaikin, A., Aumann, H. H., Lee, J., & Susskind, J. (2017). Diurnal cycle variability of surface temperature inferred from AIRS data. *Journal of Geophysical Research: Atmospheres*, 122, 10,928–10,938. <https://doi.org/10.1002/2016JD026265>

Received 17 NOV 2016

Accepted 27 SEP 2017

Accepted article online 29 SEP 2017

Published online 28 OCT 2017

## Diurnal Cycle Variability of Surface Temperature Inferred From AIRS Data

A. Ruzmaikin<sup>1</sup>, H. H. Aumann<sup>1</sup> , Jae Lee<sup>2</sup> , and Joel Susskind<sup>2</sup>
<sup>1</sup>Jet Propulsion Laboratory, California Institute of Technology, Pasadena, CA, USA, <sup>2</sup>Goddard Space Flight Center, Greenbelt, MD, USA

**Abstract** The diurnal cycle of the Earth surface temperature is investigated using the daily range of the satellite skin temperature data (DTR) provided by measurements of Atmospheric Infrared Sounder (AIRS) in 2002–2015. The AIRS is on the Aqua satellite, which is in a polar orbit with two crossing times per day at every location on the Earth. Its measurements from the ascending (day) and descending (night) orbits can serve as a proxy for the diurnal cycle. The spatial pattern of the DTR of the skin temperature and its time variability for 14 years of the AIRS operation allows to evaluate the diurnal cycle change on the decadal time scale. Using the empirical mode decomposition of the data time series, it is found that the DTR of the surface (skin) temperature over the global Earth has a temporal small positive trend in the decade of the AIRS measurements indicating that the day temperatures grew slightly more rapidly than the night temperatures. A possible cause of the observed DTR increase is a decrease of the low cloud fraction at nighttime found for the same time period from the AIRS retrievals.

**Plain Language Summary** The diurnal cycle (day-night difference) of the Earth surface temperature is investigated using the daily range of the satellite skin temperature data (DTR) provided by measurements of Atmospheric Infrared Sounder (AIRS) instrument in 2002–2015. The AIRS is on the Aqua satellite, which is in a polar orbit with two crossing times per day at every location on the Earth. Its measurements from the ascending (day) and descending (night) orbits can serve as a proxy for the diurnal cycle. It is found that the DTR of the surface temperature over the global Earth has a small positive trend in the decade of the AIRS measurements indicating that the day temperatures grew slightly more rapidly than the night temperatures. A possible cause of the observed DTR increase is a decrease of the low cloud fraction at nighttime found for the same time period from the AIRS retrievals.

## 1. Introduction

The diurnal cycle (DC) is one of the simplest most basic climate patterns resulting from the rotation of the Earth. Diurnal surface temperature response lags the incoming and outgoing radiation. Peak daily temperature occurs after noon, as air keeps absorbing the heat, and minimum daily temperature occurs after midnight due to the loss of the heat in the form of outgoing longwave radiation. As solar shortwave radiation strikes the Earth's surface each morning, a thin (1–3 cm) skin layer of air develops above the ground by conduction. Incoming solar radiation exceeds outgoing heat energy after noon to reach the equilibrium corresponding to the maximum of the DC.

The DC of the skin temperature differs over ocean from that over land and over different types of land (high deserts, planes, etc.) and depends on geographical location and seasons. Due to turbulent mixing in the upper ocean and strong solar heating, the oceanic day sea surface temperature (SST) can exceed the night SST by several degrees Celsius (cf. Stuart-Menteth et al., 2003, and references therein).

Spatial distribution and time evolution of the DC have climate implications. Karl et al. (1993) reported that in 1951–1990 the monthly mean minimum temperatures for over 50% of the Northern Hemisphere land and 10% of the Southern Hemisphere land (accounting for 37% of the global land area) have risen at a rate 3 times higher than the maximum temperatures. The diurnal temperature range (DTR) decreased at about the rate of increase in the global temperature. These authors suggested that the decreasing trend in DTR is related to the increase of cloud cover over land areas at nighttime. Vose et al. (2005) reexamined these trends using new data acquisitions covering 71% of the total global land area to confirm a significant DTR decrease

in 1950–2000 ( $-0.066^{\circ}/\text{decade}$ ). Braganza et al. (2004) evaluated the global DTR as an index of climate change and variability using observations and climate model simulations representing unforced climate variability and anthropogenic climate change. On decadal time scales, modeled and observed intrinsic variability of DTR (a negative trend  $0.4^{\circ}\text{C}$  over 50 years) compare well and were independent of variations in global mean temperature. Observed reductions in DTR over the last century were found to be large and unlikely to be due to natural variability alone. Comparison of observed and anthropogenic-forced model changes in DTR over the last 50 years showed much less reduction in DTR in the model simulations due to greater maximum temperatures in the models than observed. This difference is likely attributed to increases in cloud cover that were observed over the same period and were absent in model simulations (Braganza et al., 2004).

However, Hansen et al. (1995) found no DTR trend for the satellite era 1979–2004. They used the Goddard Institute for Space Studies global climate model to investigate the impact of a wide range of radiative forcing and feedback mechanisms on the diurnal cycle of surface air temperature attempting to rule out many potential explanations for the diurnal changes reported by Karl et al. (1993) and to infer fundamental information concerning the nature and location of the principal global climate forcings. They concluded that the large damping of the diurnal cycle of the surface air temperature implies the existence of a substantial climate forcing located in the continental regions and that anthropogenic aerosols can account for only part of this forcing; the remainder can be provided by increased cloud cover. The magnitude of the required cloud increase, 1% for low clouds, corresponds to an increase of measurement coverage of 2–5% over land (from, say, 55% to 57–60%). As stated in Hansen et al. (1995) a corollary of these results is quantitative confirmation of the idea that anthropogenic greenhouse gas warming has been substantially counterbalanced by a forced cooling. Under the assumption that the cloud change is aerosol driven, a further implication of these results is that the net rate of global warming is likely to increase substantially in coming years; the daily maximum temperature will increase by an amount not much less than the increase of the global mean temperature.

The change in the diurnal cycle can be measured using the satellite measurements that provide a global coverage of the Earth. However, infrared instruments on satellites are unable to gather data under cloudy conditions and microwave instruments have problems during precipitation. In addition, most satellites are flying in polar orbits crossing the equator twice a day at fixed local times separated by 12 h (i.e., providing only two data points in the diurnal cycle) and thus having very limited sampling of the diurnal cycle. Stuart-Menteth et al. (2003) have also shown that the spatial distribution and magnitude of diurnal temperature range (DTR) varies with the drift of the satellite orbit. In spite of these problems, satellite measurements were often used for DC evaluation especially over the ocean. Thus, 10 years of global infrared satellite data from National Oceanic and Atmospheric Administration's advanced very high resolution radiometer were analyzed by these authors to investigate global variations of diurnal temperature changes. Daily nighttime sea surface temperatures (SSTs) were subtracted from the daytime SSTs to obtain an estimate of diurnal changes of the SST (Stuart-Menteth et al., 2003). Kennedy et al. (2007) using measurements from drifting buoys at a depth of 25 cm calculated a global climatology of diurnal temperature range for 1990:2004. These means were then used to estimate the surface contribution to retrievals of tropospheric temperatures made by the Microwave Sounding Unit satellite instruments. Ignatov and Gutman (1999) analyzed monthly mean diurnal cycles (MDCs) of surface temperatures over land, represented in 3 h universal time intervals using satellite near-global data from the International Satellite Cloud Climatology Project (ISCCP) with a  $(280\text{ km})^2$  resolution (C-2 product). The MDCs have been converted to local solar time, refined to a regular 1 h time grid using cubic splines and subjected to principal component analysis. The first two modes approximate MDCs in air and ground-satellite temperatures with standard deviations of  $\approx 0.5^{\circ}\text{C}$  and  $1^{\circ}\text{C}$ , respectively, and these accuracies are improved by 20% to 35% if the third mode is added. This suggests that two to three temperature measurements during the day allow reconstruction of the full MDC and that for two modes optimal observation times are close to the occurrence of minimum and maximum daily temperatures.

Here we identify the spatial pattern and time evolution of the diurnal temperature range using the skin temperature retrieved from the satellite measurements by the AIRS instrument on Aqua satellite launched in 2002. In addition to the global pattern, we mask the data into land and ocean areas, as well the areas on the Earth with the largest diurnal cycles, such as the deserts.

Section 2 describes the data used in our study. Section 3 introduces the method of data analysis. Section 4 presents the observed spatial distribution and time variability of the DTR of the AIRS skin temperature.

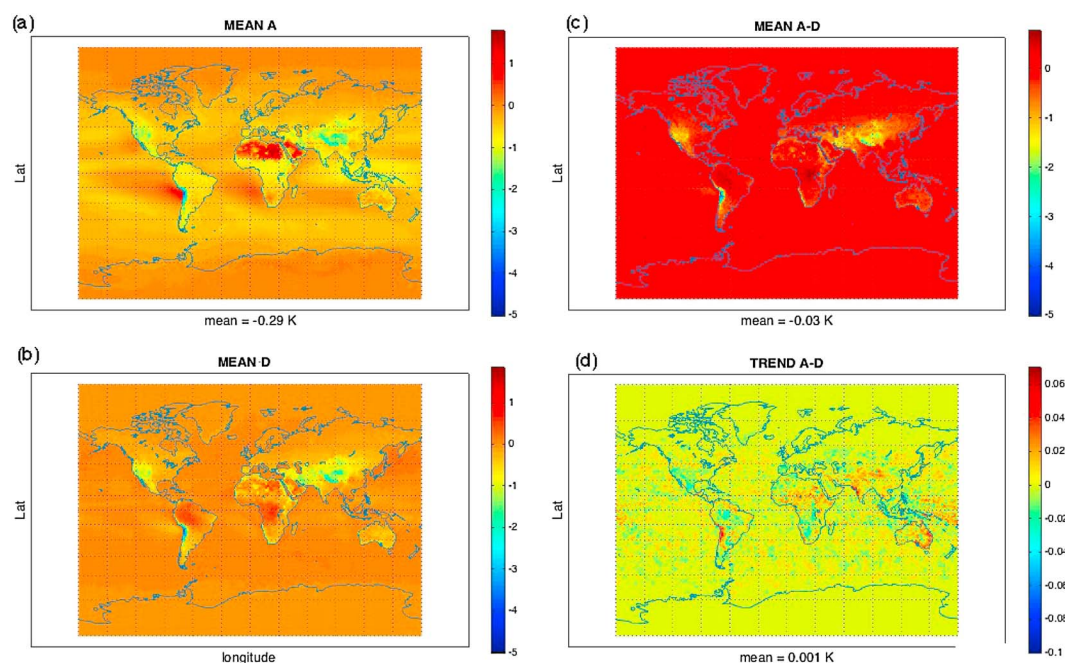


**Figure 1.** The maps of the computed (after the retrievals) versus observed differences of the surface brightness temperature for (a) the day (ascending orbits, A), (b) night (descending orbits, D), (c) the day-night difference, and (d) the trend map of the diurnal differences. The global means are shown under each panel. The linear global mean trend for the DTR and its error (estimated by bootstrapping the data) are found to be  $0.001 \pm 0.007$  K/yr. The regions with higher trends (intense red) occupy a small portion of the globe (mostly deserts, mountains, and ocean areas with a lot of low clouds).

In section 5 we discuss the variability of the DTR over global land, ocean, and areas on Earth with the largest diurnal changes. Section 6 presents a summary and a short discussion of the results.

## 2. Data

We will use the skin temperature retrieved at Level 2 (version 6) from the measurements by the Atmospheric Infrared Sounder (AIRS) on the Aqua satellite in 2002–2015. AIRS has been in a stable (nondrifting) orbit for the past 14 years with the expectation of a 20 year lifetime. The AIRS absolute calibration accuracy and stability have been well documented (Aumann et al., 2003, 2012). AIRS was launched in May 2002 on the EOS Aqua satellite into a 705 km altitude Sun-synchronous,  $98^\circ$  inclination circular orbit. We refer to the 1:30 p.m. ascending node as the “day” overpass and to the 1:30 a.m. descending part of each orbit as the “night” overpass (Figure 1). The ascending node and altitude of the orbit are actively maintained. The AIRS footprint subtends an angle of  $1.1^\circ$ . The footprints are scanned  $\pm 49.5^\circ$  cross track resulting in a 1,650 km wide swath. The footprint geometrical size on the ground increases from a round spot of 13.5 km diameter at nadir to a  $99 \text{ km} \times 23 \text{ km}$  ellipse at the extreme scan angles, with an average 30 km size averaged over all scan angles. The global coverage allows us to separate the evolution of temperature over the ocean and land areas expanding the over land studies of the DTR change.

The error estimation for the surface temperature depends on the region and can be found in the AIRS mission document “V6 L2 Quality Control (QC) and Error Estimation.pdf” on the website <http://disc.sci.gsfc.nasa.gov/AIRS>. The surface temperature error estimates called TSurfStdErr, for the quality cases QC = 0 (best) and QC = 1 (good) over ocean, are less than 1.1 K. It is less than 1.4 K for latitudes lower than  $-40^\circ$ . For latitudes lower than  $-60^\circ$  TSurfStdErr is larger but less than 2.0 K. Over land and frozen regions, TSurfStdErr is less than 7 K. Over ocean the quality control attempts to identify only good cases. Over land a large selection of cases are marked as “good” to ensure adequate coverage for production of monthly means for climate studies. All these errors are smaller than the diurnal variability of the AIRS skin temperature.

Hearty et al. (2014) provided estimates of the sampling biases of climatologies derived from the AIRS instrument. The instrumental sampling biases are mainly caused by clouds. They are up to 2 K cold and more than



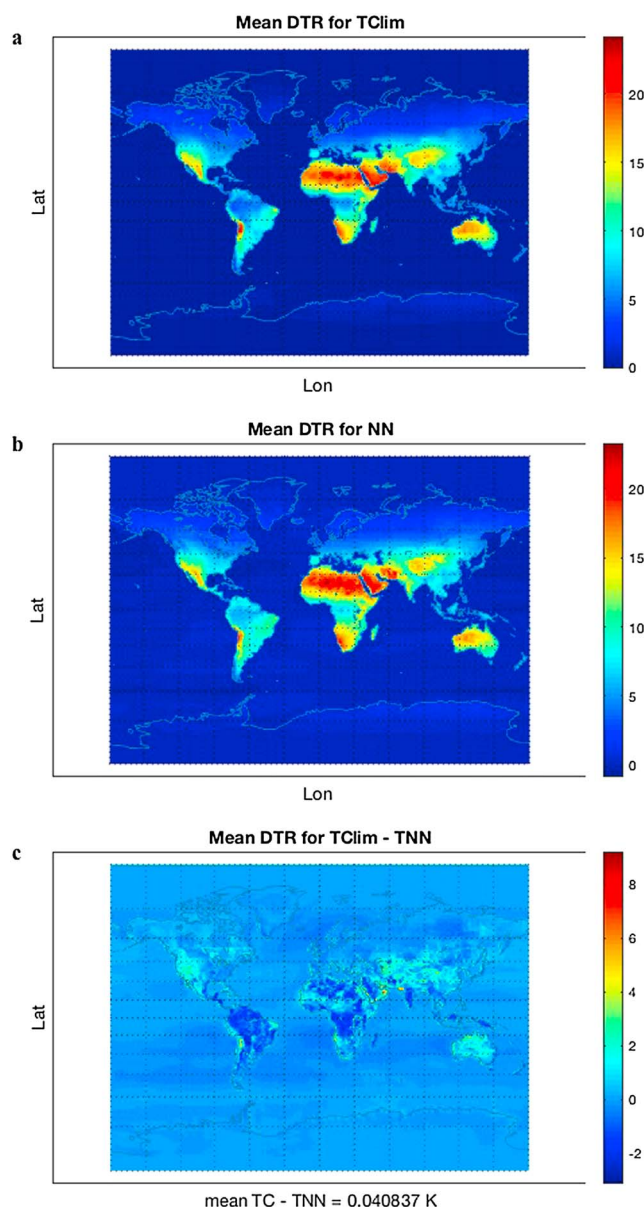


**Figure 2.** The AIRS retrieved (a) climatological skin temperature versus the (b) neural network (first guess) temperature and (c) their difference.

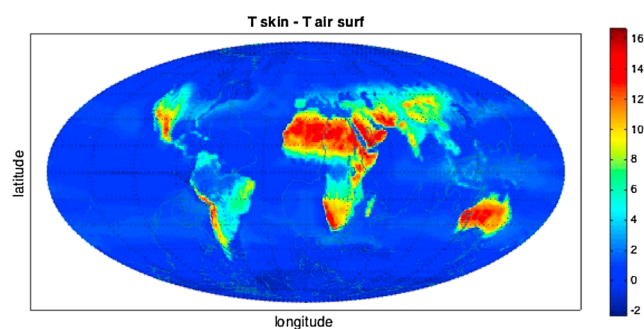


**Figure 3.** The difference between the skin temperature and the surface air temperature retrieved from AIRS measurements. The maximum differences are seen over land, for example, in Africa and Australia.

30% dry over midlatitude storm tracks and tropical deep convective cloudy regions and up to 20% wet over stratus regions. Other factors such as surface emissivity and temperature can also influence the instrumental sampling bias over deserts where the biases can be up to 1 K cold and 10% wet.

The AIRS retrievals involve a cloud-clearing algorithm. Clouds are usually the largest source of errors in the retrievals of the satellite data. To test how the AIRS surface temperature errors associated with clouds are “cleared” for the day and night data, we use a variable “CBTmOBT” from the AIRS research products (Figure 1). This variable compares the calculated cloud-cleared retrieval for the surface brightness temperature with the directly observed brightness temperature in the window channel  $1,231\text{ cm}^{-1}$ . Although there are substantial differences in some, especially land areas, the differences in the retrieved and observed temperatures were found to be small after averaging over the globe and the whole ocean and land areas (0.001 K for the global map, 0.013 K for the ocean, and 0.04 K for the land) justifying our trend results, at least for the global case.

We use the latest AIRS version 6 retrievals that adopt a neural-net first guess, which contains very accurate low-level temperature profile fine structure (Milstein & Blackwell, 2016). To test how this first guess could influence the DTR, we generated the global maps of the DTR for the  $T$  skin climatology and compare it with the global map constructed out of the neural network temperature (Figure 2). Although there are substantial differences in some areas, the global difference is found to be very small (0.04 K).

Since most of previous studies of DTR used the surface air temperature, we note that AIRS retrievals generate two standard surface temperature products: surface skin temperature,  $T_{\text{skin}}$ , and surface air temperature,  $T_a$ . The surface skin/surface air temperature difference is defined (Susskind et al., 2014) as follows:

$$\Delta T_{s,a} = T_{\text{skin}} - T_a(\text{ps}),$$

where ps is the surface pressure.  $\Delta T_{s,a}$  can be used as a parameter with regard to the understanding of the sensible heat flux between Earth’s surface skin and its atmosphere. AIRS radiances are sensitive to changes in  $T_{\text{skin}}$ , which is derived simultaneously with shortwave spectral emissivity and spectral surface bidirectional reflectance using AIRS channels between  $2,396\text{ cm}^{-1}$  and  $2,665\text{ cm}^{-1}$ . On the other hand, AIRS radiances are not sensitive to changes in  $T_a(\text{ps})$  very near the surface. AIRS version 6 generates reasonable values of  $T_a(\text{ps})$  because the neural-net first guess contains very accurate low-level temperature profile fine structure.  $T_a(\text{ps})$  is determined so as to make the best match to the radiances for the channels used in the  $T_a(\text{ps})$  retrieval process. If  $T_{\text{skin}}$  is too warm (cold), this would make radiances too high (low) for a given  $T_a(\text{ps})$ , the solution would tend to lower (raise) values of  $T_a(\text{ps})$  to compensate for the error in  $T_{\text{skin}}$ . Therefore, errors in  $T_{\text{skin}}$  would tend to produce errors in  $T_a(\text{ps})$  of the opposite sign and consequently degrade  $\Delta T_{s,a}$ . Susskind et al. (2014) compared seasonal mean climatologies of  $T_{\text{skin}}$ ,  $T_a(\text{ps})$  and their difference for the ascending (daytime) and descending (nighttime) orbital data. It is found that annual mean surface skin temperature is about 1 K warmer than the surface air temperature over land, especially in arid areas for day time (1:30 p.m.) with opposite sign of difference for the nighttime (1:30 a.m.). Oceanic surface skin temperatures also tend to be warmer than surface air

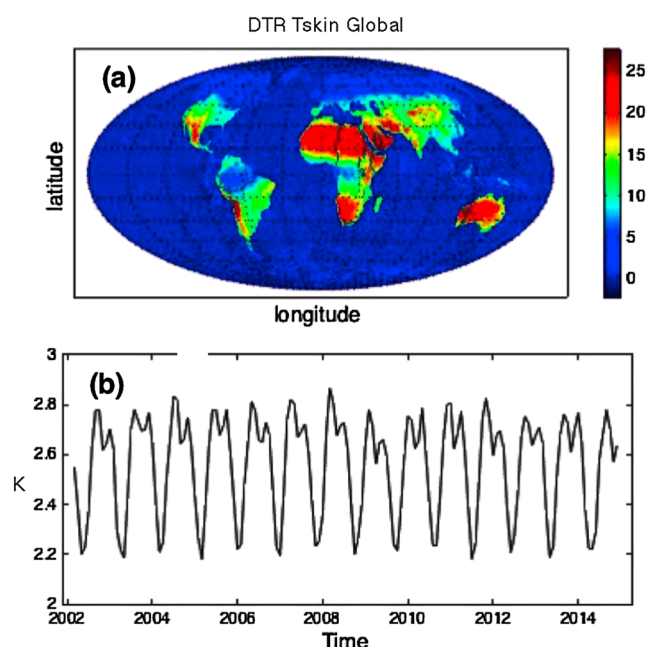


**Figure 4.** (a) Spatial distribution of the global mean DRT of the AIRS skin temperature data. (b) Time variability of the global DRT of the AIRS skin temperature.

oscillating in time and a nonoscillating residual. The number of modes is determined by the data, that is, EEMD is data adaptive, and, in contrast to Fourier spectral decomposition, it does not require stationarity of the data. As such, it is well suited for the analysis of nonstationary and nonlinear time series. The IMF characteristic time scales are determined by the data itself. Each IMF represents a mode of oscillation with time-dependent amplitude and frequencies that lie within a narrow band, the center of which defines the mean period of the mode. The process of extracting the individual modes or essential scales from the data is called sifting and is performed many times to produce a single IMF. In this process local maxima and minima are identified in the record and envelopes are formed by fitting cubic splines to the extreme values. The differences between the envelope and the mean provide an estimate of the first IMF component. Once the first IMF has been obtained, it is subtracted from the original data, and process is repeated to get the next IMF mode till it comes to the nonoscillating residual, which is treated here as a trend on decadal time scale. One known problem in the application of the nonensemble EMD is that mode mixing occurs when a time series includes intermittently occurring signals of widely separated time scales, that is, when a high-frequency signal in one time interval is followed by a smooth, low-frequency signal in the following time interval. In order to address this problem, Wu and Huang (2009) have developed a noise-assisted technique called an ensemble EMD, or EEMD, which defines the true IMF as the mean of an ensemble of IMFs. An ensemble member consists of the signal plus white noise time series of the same length. By creating an ensemble of IMFs, it is possible to generate IMFs, each of which has a narrow frequency band, which essentially do not overlap with the frequencies that are contained in adjacent IMFs. Here we will typically apply the EEMD with 150–300 ensemble members and checked that the increase of the ensemble number does not substantially change the results. Each IMF not necessarily describes a real physical variability at its time scale. Adding attributions to the IMF oscillations is needed to put it in context of the real variability such as seasonal oscillations or a climate trend.

Due to the time variability on many time scales, the definition of trend, as determined by the EEMD, requires a clarification. The EEMD modes are selected by progressive time-variant data-adaptive filtering. The oscillating modes have zero mean values. The modes with nonzero mean are combined into a nonoscillating residual, which typically growing or decreasing in time. Whether this residual defines a secular trend or is just a long-term nonstationary component of the data given at a finite time interval remains unclear. The modes obtained using this method do not reflect the actual physical processes out of which the data are formed. However, it is important to note that the proxy for trend extracted by the EEMD is adaptive and intrinsic since it is derived from the data without the need of introduction of any extra functions in addition to the data, such as linear or polynomial functions used in data fitting. In any case a mode attribution to a real physical

temperatures in the midlatitudes for all times. Polar surface skin temperatures are colder than surface air temperatures (by about 1 K) except over open ocean. The mean difference between the two AIRS products  $T_{\text{skin}}$  and  $T_a(\text{ps})$  is shown in Figure 3. The maximum differences are seen over land, especially in the North and South Africa, Arabian deserts, and Australia.

Although AIRS provides only two points on the diurnal cycle, these points are well positioned near the daily minimum and maximum temperature (cf. Figure 1 in Kennedy et al., 2007). We will use the difference between these points as a proxy for the diurnal temperature range (DTR). We use the version 6 of AIRS L3 jointly temperature–water vapor retrieved monthly data for the skin temperature in 2002–2016 presented on  $1^\circ \times 1^\circ$  latitude–longitude grid. The data can be downloaded from the Goddard Space Flight Center archive at <http://disc.sci.gsfc.nasa.gov>.

### 3. The Method of Data Analysis

To carry out the variability and trend analysis, we apply the data adaptive ensemble empirical mode decomposition (EEMD) technique (Wu & Huang, 2009) to identify the oscillating modes of the DTR and its nonoscillating residuals (trends) (Wu et al., 2011) over the global Earth and over land and ocean areas. The methodology of the EEMD is described in detail by Wu and Huang (2009). The EEMD is a method of decomposing a time series into a sequence of empirically orthogonal intrinsic mode functions (IMF)

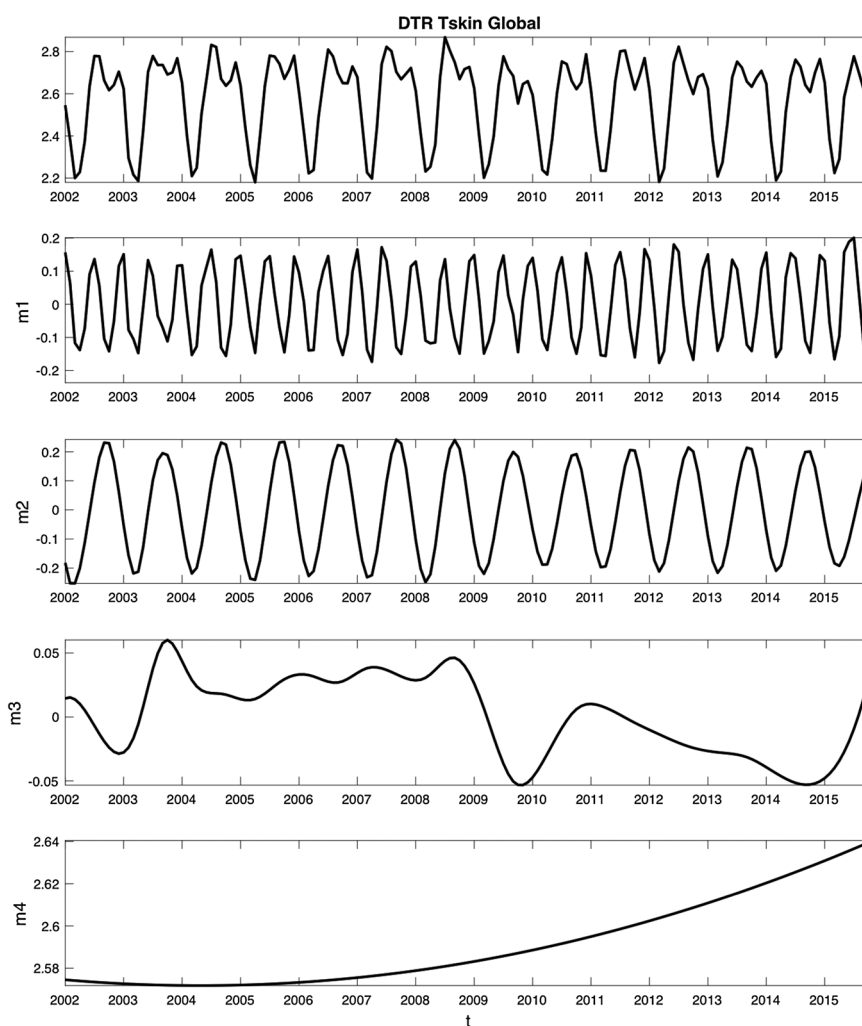


**Figure 5.** The empirical mode decomposition of the variability of the global DRT (combining land and ocean) for the skin temperature. Modes 1 and 2 show the semiannual and annual variability. Modes 3–6 display the interannual variability. The last mode, a residual shows a change of about 0.07 K in 14 years of the AIRS measurements (positive decadal trend). The linear trend fit to the residual gives an estimate  $5 \pm 0.3$  mK/yr. The linear trend determined directly from the data ( $5 \pm 5.6$  mK/yr) is not significant.

process is always required. Since all data always contain noise, it is important to test whether an IMF is a true signal or only a component of noise. Wu et al. (2011) suggested a method to characterize statistical significance of the IMF by comparing their energy (determined by their standard deviations of the IMF time series at each time scale) dependence on the mean periods of the IMFs with the mean period-energy dependence for the white noise. (The expansion of the method to color noise can be found in Flandrin et al., 2004.) We used this test for our study of the cases described below.

#### 4. The Distribution and Variability of the Global DTR

Figure 4 shows the spatial distribution of the global diurnal temperature range (DTR) averaged over 2002–2015 (a) and its time variability (b) obtained from the AIRS skin temperature differences for ascending and descending orbits in every grid point on the globe. The largest DRTs are seen over the land in the desert areas, and the DRT is minimal over the ocean.

To analyze the time variability presented in Figure 4b, we apply the EEMD method described in the previous section. This decomposition of the data allows separation of oscillating modes from a nonoscillating residual defining a proxy for the trend on decadal time scale (Figure 5). The direct decomposition results in seven modes. These modes are found to be statistically significant at 90% level of significance. For better



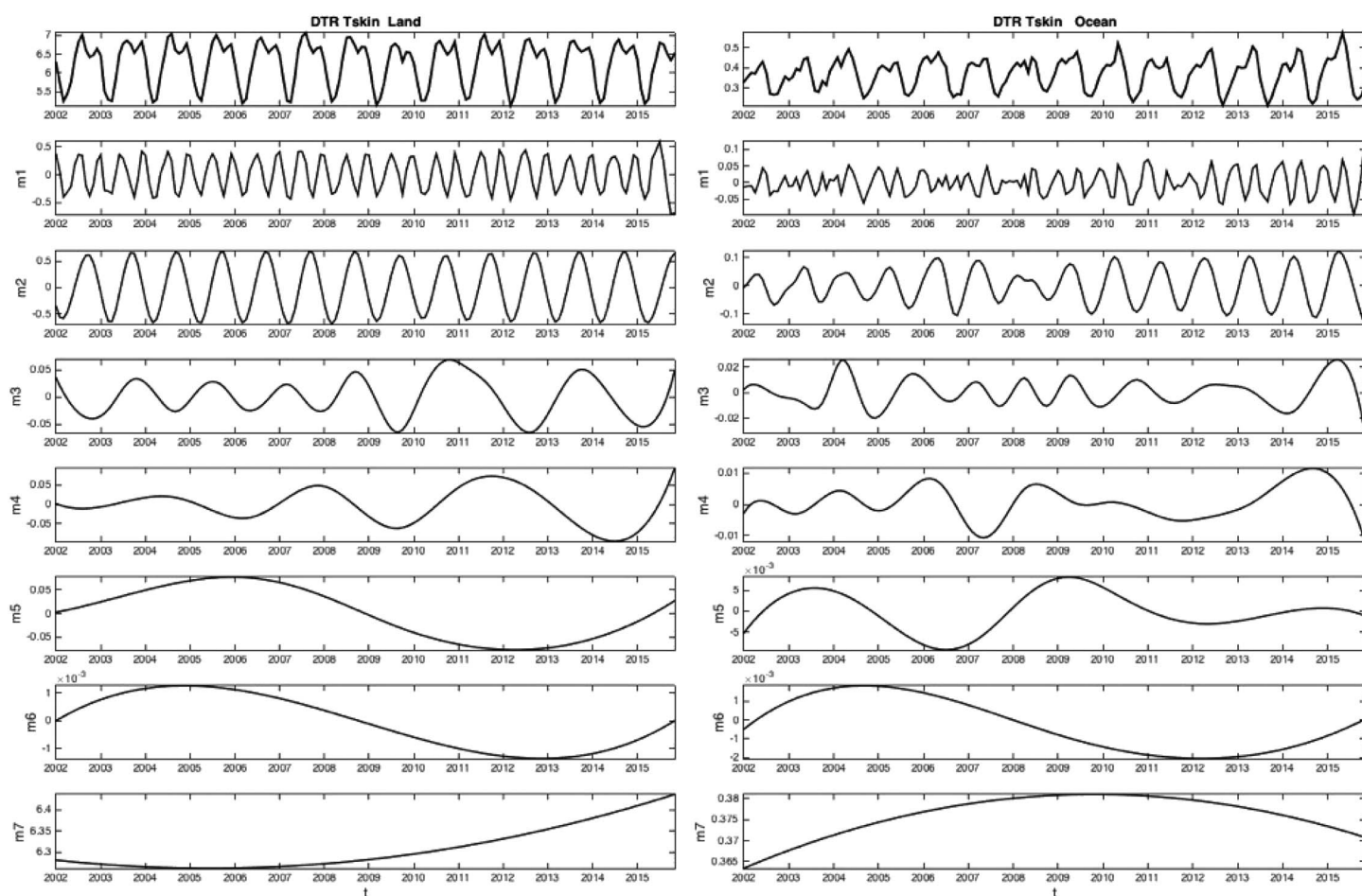


**Figure 6.** The empirical mode decomposition of the skin temperature for (left column) global land. The linear trend for the residual is  $10 \pm 0.04$  mK/yr. The linear trend determined directly from the data ( $2 \pm 10$  mK/yr) is not significant. (right column) Global ocean. The linear trend determined directly from the data ( $6 \pm 10$  mK/yr) is small and not statistically significant.

interpretation we combine the modes with a time variability larger than a year into one mode (now IMF mode 3). The first mode displays the seasonal variability, the second mode is the annual variability and the combined third mode, which has mostly nonlinear variations, characterizes the multiyear variability of the DTR. For example, we see the apparent impacts of weak El Niño in 2002–2003 and 2004–2005 and strong El Niño in 2009–2010 and 2015. The residual (the fifth panel) has a positive trend, that is, the DTR averaged over the globe is increasing in time interval when the AIRS measurements were made. The residual slowly increases by 0.07 K over 14 years (about 0.05 K/decade = 0.005 K/yr) according to the lapse of the residual. A linear trend directly fitted to the  $T_{\text{skin}}$  data in Figure 5 (first panel) is found to be insignificantly small but also positive (0.003 K/yr). The separate decompositions of the day and night skin temperatures (not shown) demonstrate that the day trend is slightly higher than the night trend confirming the sign of the DTR trend seen in Figure 5.

### 5. DTR Variability Over Land, Ocean, and Hot Deserts

To further understand the DC variability and compare it with the earlier studies that used the land (ground) data, we consider the DC separately for the data averaged over the global land and over the global nonfrozen ocean.

Figure 6 shows the EEMD decomposition of the AIRS skin temperature over global land and global ocean. Following Karl et al. (1993), we excluded the polar regions (beyond  $70^\circ$  latitudes). The residual over land has a positive trend on the decadal time scale, while the DRT residual over ocean is not monotonic. The  $T_{\text{skin}}$  trend over the ocean stalled in 2009–2011 (at the time of the transition from El Niño to La Niña) and changed



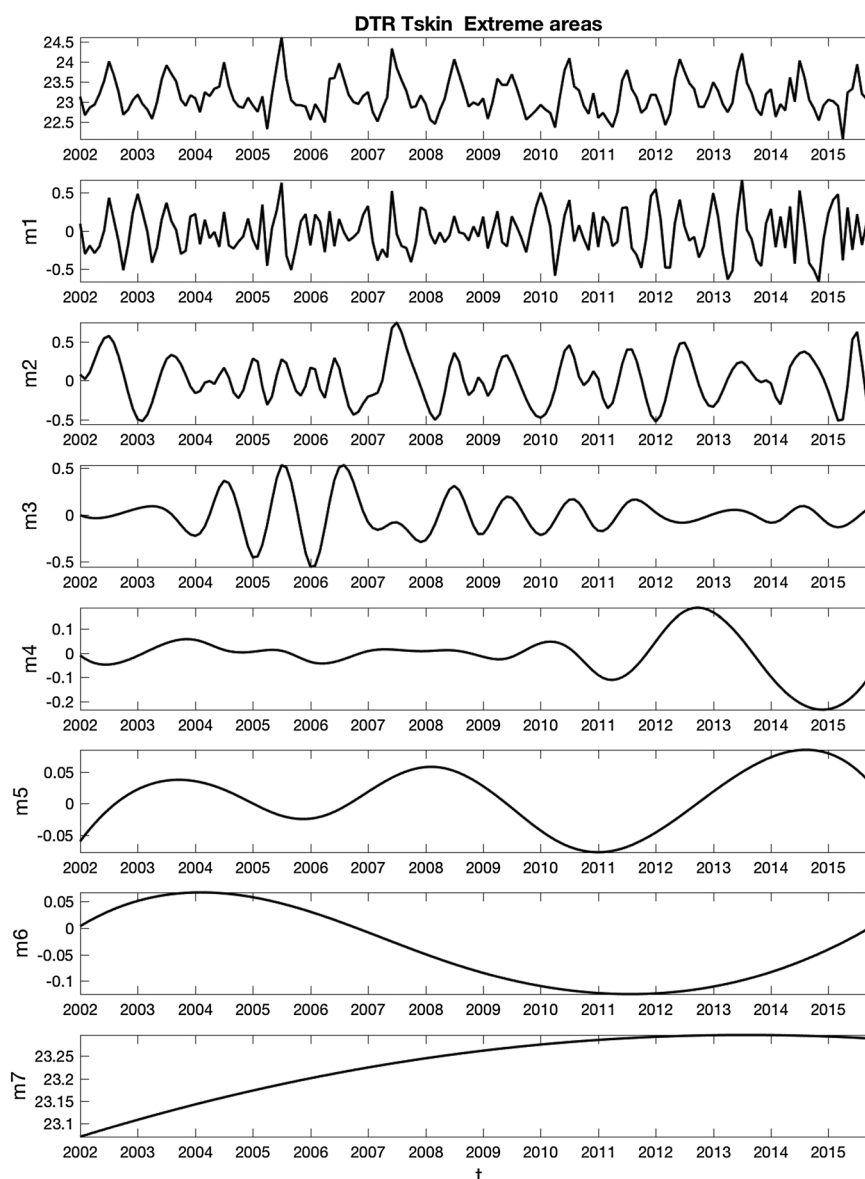


**Figure 7.** The empirical mode decomposition of the skin temperature for areas with extreme diurnal cycle (DTR exceeding 20 K). The residual increased by 0.35 K within 14 years.

the sign. The  $T_{\text{skin}}$  over the ocean varies more chaotically although there is a similar interannual variability mode over the land and ocean displayed in EEMD mode 6. From the last left panel of this figure we see a positive change of about 0.2 K in 14 years roughly corresponding to a small trend for the land DRT of  $\approx 0.14$  mK/yr.

The variability and the residual for the skin temperature over the areas with the largest DTR over land (DTR exceeding 20 K) are shown in Figure 7. In contrast to the global distribution, the DTR in the extreme areas raised up from 2002 to 2012, passed through maximum and started decreasing after 2014.

## 6. Discussion

Using the satellite data from AIRS measurements in 2002–2016, we find that the globally averaged daily range of the satellite skin temperature data (DTR) was increasing during this time period. Similar positive trend on decadal time scale is found over the land-only area. This change is in reverse to the earlier reported secular decrease in diurnal cycle of the land temperature for the time period 1951–1990 (Karl et al., 1993). Using the ensemble empirical mode decomposition of the data time series, it is found that the DTR of the surface (skin)

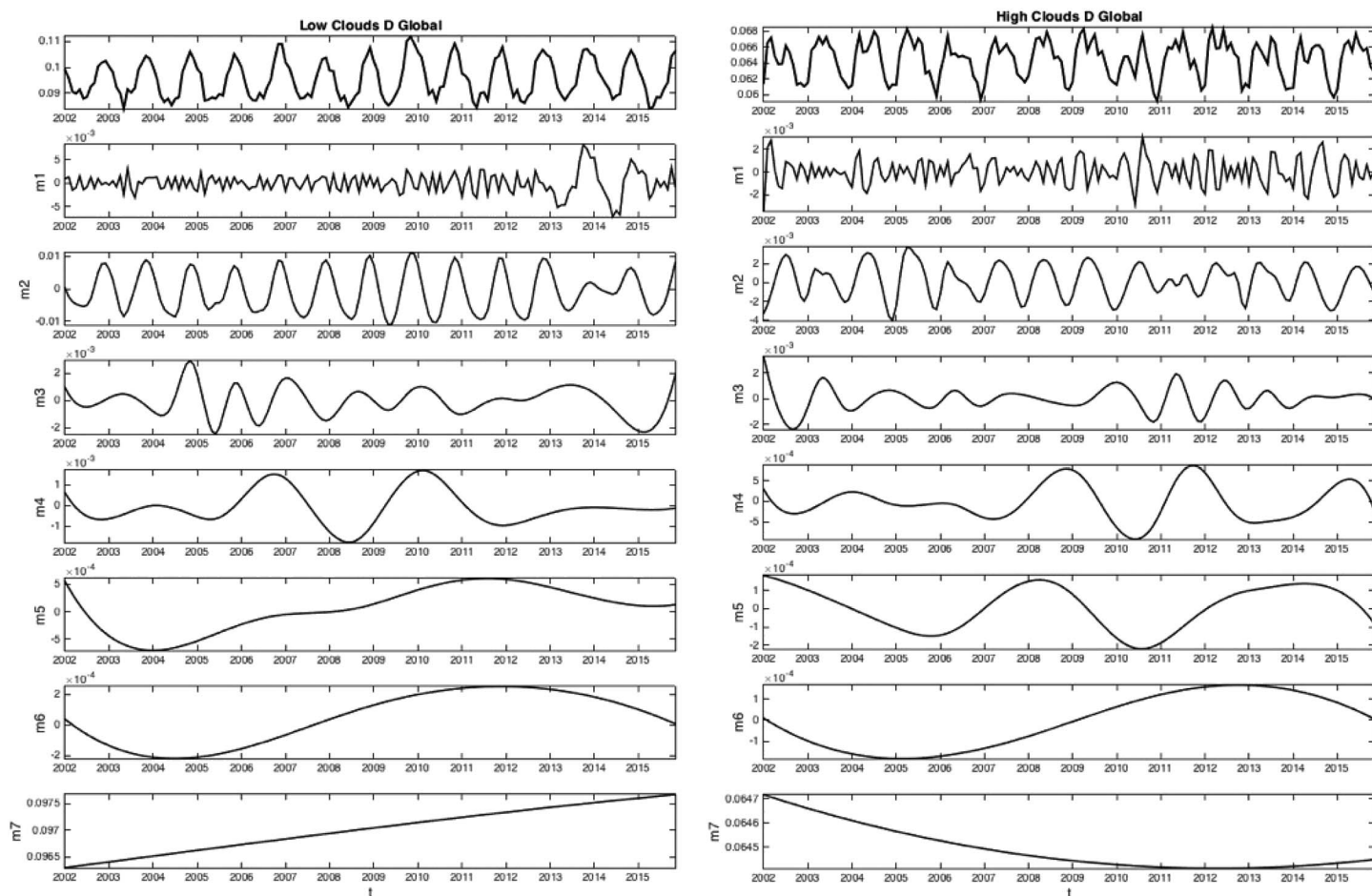


**Figure 8.** The empirical mode decomposition of the cloud fraction for (left column) low clouds and (right column) high clouds over the global Earth for descending (night) orbits as determined from the v6 version of the AIRS L2 retrievals. The residual of the low clouds increase by 0.12 mK within 14 years. The direct fit to linear trend for the residual for the low clouds gives  $1 \pm 0.1$  mK/yr. The residual of the high clouds in the same time period decreased by 0.3 mK. The linear trends for clouds determined directly from the data are not statistically significant.

temperature over the global Earth has a temporal small positive rise in the decade of the AIRS measurements, indicating that the day temperatures grew slightly more rapidly than the night temperatures. A possible cause of the observed DTR increase is a decrease of the low cloud fraction at nighttime found for the same time period from the AIRS retrievals.

A small magnitude of the proxy for the DTR decadal trends found here rises a question on how reliable is our estimate of the DTR variability and the decadal trend, especially in view of the facts that the 14 year AIRS record is certainly too short of a time period for determining any secular trend related to climate change and the AIRS skin temperature has been retrieved with errors, in particular, over the land areas. First, what we call the decadal trend is actually a low-frequency change in DTR on decadal time scale and may nothing to do with a possible secular trend. A secular trend in the surface temperature has apparently been determined by Karl et al. (1993) who used a half-century-long data record. Second, although all trends determined directly from the 14 years of the AIRS surface temperature records are found not to be statistically significant, the ensemble empirical mode decomposition applied for our data analysis allows to extract the modes of variability from the highly noisy data giving some credit to the surface temperature changes on the decadal time scale found here.

### 6.1. On Possible Causes of DTR Changes

What drives these changes in the surface temperature? The EEMD decomposition made for the low and high clouds at nighttime retrieved from the AIRS descending orbit data for the same time period (Figure 8) shows a negative trend for low clouds, indicating that the cloud decrease could cause the rise of the DTR. A small negative trend (at the level of percent per decade) in the global low cloud fraction was reported

by Noris and Evan (2015) based on the use of ISCCP, PATMOS-x, and Moderate Resolution Imaging Spectroradiometer (MODIS) data after removal of artifacts in their cloud records. On the other hand, the fraction of the high clouds retrieved by AIRS was decreasing (last right panel in Figure 8) following the global warming. King et al. (2013) analyzed cloud properties retrieved from the Moderate Resolution Imaging Spectroradiometer (MODIS) over 9 years from daily measurements on Aqua satellite (which carries the AIRS instrument) and over 12 years of continuous daily observations on Terra satellite, which was taking data at 10:30 a.m. They found a distinctive seasonal cycle over land with much reduced seasonal variation over ocean and only a small trend in the difference between the cloud fraction retrieved from measurements on these two satellites. Thus, in agreement with the previous studies, such as Karl et al. (1993), a possible cause of the DTR trend (positive in our case) is the decrease of the low cloud cover in the same decade 2002–2016 (see the last left panel in Figure 8).

Is the change in DTR and related cloudiness anthropogenic or natural? We see that the change of the DTR trend from negative in the second part of the 20th century Karl et al. (1993) to positive in the beginning 21st century followed a similar change of the change sign of the major climate mode, the Pacific Decadal Oscillation (PDO) (cf. the PDO record at "jisao.washington.edu/pdo"). It is interesting to note that another major climate pattern, the Atlantic Multidecadal Oscillation, changed its sign from negative to positive at the transition from 20th to 21st century (see <https://en.wikipedia.org/wiki/AMO>). The time period covered by the AIRS measurements coincides with one of the time intervals of low global temperature trend (Meehl et al., 2014; Tung & Zhou, 2013). However, it remains to be investigated how the low global trend affected the trend in diurnal cycle of the surface temperature. In other words, to what extent the trends in DTR reflect the natural variability of the climate?

In contrast to the global and over land distributions, the DTR over the global ocean and in the extremely hot areas of the Earth is found to be nonmonotonic. The DTR over these regions increased from 2002 to 2010 (2012 for the hot land areas), reached maxima, and started a decrease. This behavior might be associated with the transition from the El Niño to La Niña.

# Acknowledgments

We are grateful to three reviewers for helpful critical comments. This work was supported in part by the Jet Propulsion Laboratory of the California Institute of Technology, under a contract with the National Aeronautics and Space Administration. The AIRS data used in this paper can be loaded from the website <http://disc.sci.gsfc.nasa.gov/AIRS>. Additional data are available in the cited references or included in the figures.

# References

- Aumann, H. H., Chahine, M. T., Gautier, C., Goldberg, M., Kalnay, E., McMillin, L., ... Susskind, J. (2003). AIRS/AMSU/HSB on the Aqua mission: Design, science objectives, data products and processing systems. *IEEE Transactions on Geoscience and Remote Sensing*, 41(2), 253–264.
- Aumann, H. H., Elliott, D., & Strow, L. L. (2012). Validation of the radiometric stability of the Atmospheric Infrared Sounder. In J. Buttler, X. Xiong, & X. Gu (Eds.), *Proc. SPIE Optics and Photonics Conference, Session 8510*. San Diego: Earth Observing System XVII.
- Braganza, K., Karoly, D. J., & Arblaster, J. M. (2004). Diurnal temperature range as an index of global climate change during the twentieth century. *Geophysical Research Letters*, 31, L13217. <https://doi.org/10.1029/2004GL019998>
- Flandrin, P., Rilling, G., & Goncalves, P. (2004). Empirical mode decomposition as a filter bank. *IEEE Signal Processing Letters*, 11, 112–114. <https://doi.org/10.1109/LSP.2003.821662>
- Hansen, J., Sato, M., & Ruedy, R. (1995). Long-term changes of the diurnal temperature cycle: Implications about mechanisms of global climate change. *Atmospheric Research*, 37, 1175–209.
- Hearty, T. J., Savtchenko, A., Tian, B., Fetzer, E., Yung, Y. L., Theobald, M., ... Won, Y.-I. (2014). Estimating sampling biases and measurement uncertainties of AIRS/AMSU-A temperature and water vapor observations using MERRA reanalysis. *Journal of Geophysical Research: Atmospheres*, 119, 2725–2741. <https://doi.org/10.1002/2013JD021205>
- Ignatov, a., & Gutman, G. (1999). Monthly mean diurnal cycles in surface temperatures over land for global climate studies. *Journal of Climate*, 12, 1900–1910.
- Karl, T. R., Jones, P. D., Knight, R. W., Kukla, G., Plummer, N., Razuvayev, V., ... Peterson, T. C. (1993). Asymmetric trends of daily maximum and minimum temperature. *Bulletin of the American Meteorological Society*, 74(6), 107–123.
- King, M. D., Platnick, S., Menzel, W. P., Ackerman, S. A., & Hubanks, P. A. (2013). Spatial and temporal distribution of clouds observed by MODIS onboard the Terra and Aqua satellites. *IEEE Transactions on Geoscience and Remote Sensing*, 51(7), 3826–3852.
- Kennedy, J. J., Brohan, P., & Tett, S. F. B. (2007). A global climatology of the diurnal variations in sea-surface temperature and implications for MSU temperature trends. *Geophysical Research Letters*, 34, L05712. <https://doi.org/10.1029/2006GL028920>
- Meehl, G., Teng, H., & Arblaster, J. M. (2014). Climate model simulations of the observed early-2000s hiatus of global warming. *Nature Climate Change*, 4, 898–902.
- Milstein, A. B., & Blackwell, W. J. (2016). Neural network temperature and moisture retrieval algorithm validation for AIRS/AMSU and CrIS/ATMS. *Journal of Geophysical Research: Atmosphere*, 121, 1414–1430. <https://doi.org/10.1002/2015JD024008>
- Stuart-Menteth, A. C., Robinson, I. S., & Challenor, P. G. (2003). A global study of diurnal warming using satellite-derived seasurface temperature. *Journal of Geophysical Research*, 108(C5), 3155. <https://doi.org/10.1029/2002JC001534>
- Noris, J. R., & Evan, A. T. (2015). Empirical removal of artifacts from the ISCCP and PATMOS-x satellite cloud records. *Journal of Atmospheric and Oceanic Technology*, 32, 691–702.
- Susskind, J., Lee, J., & Iredell, L. (2014). Version 6 Surface Skin/Surface Air Temperature Differences and their Interannual Variability, report at NASA Sounder Science Team Meeting. Retrieved from [airs.jpl.nasa.gov/events](http://airs.jpl.nasa.gov/events)
- Tung, K. K., & Zhou, J. (2013). Using data to attribute episodes of warming and cooling in instrumental records 2004. *Proceedings of the National Academy of Sciences of the United States of America*, 110, 2058–2063.

- Vose, R. S., Easterling, D. R., & Gleason, B. (2005). Maximum and minimum temperature trends for the globe: An update through 2004. *Geophysical Research Letters*, 32, L23822. <https://doi.org/10.1029/2005GL024379>
- Wu, Z., & Huang, N. E. (2009). Ensemble empirical mode decomposition: A noise-assisted data analysis method. *Advances in Adaptive Data Analysis*, 1, 1–41.
- Wu, Z., Huang, N. E., Wallace, J. M., Smoliak, B., & Chen, X. (2011). On the time-varying trend in global-mean surface temperature. *Climate Dynamics*, 37, 759–773. <https://doi.org/10.1007/s00382-011-1128-8>